Bioorthogonal Antigens

Pawlak, J.B.

3

The optimization of bioorthogonal epitope ligation within MHC-I complexes

Published as part of: Joanna B. Pawlak, Brett J. Hos, Michel J. van de Graaff, Otty A. Megantari, Nico J. Meeuwenoord, Herman S. Overkleeft, Dmitri V. Filippov, Ferry A. Ossendorp and Sander I. van Kasteren.
ACS Chemical Biology, 2016, 11(11): 3172-3178.
Silvia Pujals Riatos and Lorenzo Albertazzi also contributed to the work described in this chapter.

3.1 Introduction

The first step of determining whether bioorthogonal antigens could serve as a method for studying the entirety of the cross-presentation pathway, was to determine what the parameters were under which bioorthogonal ligations could be performed on the surface of the cell. If successful, bioorthogonal variants of antigens could then be used to allow the quantification of epitope peptides, independent of T cell reagents. At present, reagents are mostly available for the study of known specific peptides, for example by using T cells specific for particular peptide-MHC-I (pMHC-I)[1], recombinant T cell receptors (TCRs)[2], or TCR-like antibodies specific for a given pMHC-I[3].

It was hypothesized that bioorthogonal peptides would allow the quantification of the surface concentration in MHC-I complexes by specifically incorporating bioorthogonal functional groups in tolerated positions in epitopes, followed by an on-cell ligation reaction with a non-cell permeable reporter. This would mean, the epitope could be quantified independent of T cell-based reagents, which would for example greatly facilitate the study of pMHC-Is for which TCR-based reagents are not available. Unlike larger detectable groups, bioorthogonal groups are small enough not to affect MHC

loading. Furthermore, their *in vivo* stability[4] makes them potentially suited to the study of pMHC-I complexes on the surface of the cell[5].
Quantification of the bioorthogonal antigens can be achieved by ligation of a complementary fluorophore to the bioorthogonal amino acid side chain at the end of the experiment. That is however quite challenging, due to the low numbers of specific pMHC-Is available on the cell surface. Typically, only 10^5-10^6 MHC-I molecules are present per cell[6] which are loaded with multiple different self-peptides. The detection of a specific subset of peptide loaded MHC-Is would thus require sensitive and selective ligation of these peptides. Furthermore, these ligations have to be done on peptides within MHC-I complexes, adding to the experimental stringency.
This chapter reports the optimization of the bioorthogonal quantification of peptides loaded on MHC-I complexes. The binding and ligation parameters that allow the quantification of exogenous bioorthogonal epitopes within a pMHC-I complex were established. The effect of bioorthogonal modification of epitopes on MHC-I binding, TCR-recognition and bioorthogonal reaction efficiency in various possible ligation reactions to facilitate further translation to the quantification and imaging of the antigen presentation pathway was optimized and assessed.

3.2 Results and discussion

The first requirement for bioorthogonal epitopes to be of use in the study of pMHC-Is is that the modification itself must not negate binding to MHC-I. Once bound to MHC-I, the steric hindrance should be sufficiently small to allow on-surface ligation of the bioorthogonal group to allow the quantification of the pMHC-I preferably below MHC-I saturation levels.

Bioorthogonal modification and pMHC-I stability

It was first determined whether bioorthogonal chemical functionalities could be incorporated into minimal MHC-I epitopes without affecting binding to the MHC-I. Initial focus was on the two smallest available bioorthogonal groups with the lowest side-reactivity: the alkyne and azide[7]. Both minimally impact structure due to their small size and bioorthogonality, and are readily incorporated into peptides[8] and proteins[9] in the side-chain modified amino acids azidohomoalanine (Aha, **1**, Figure 1) and propargylglycine (Pg, **2**, Figure 1). Furthermore, they have exceptional stability profiles as only very few biological sequestration reactions of alkynes[10] and azides[11] have been reported.

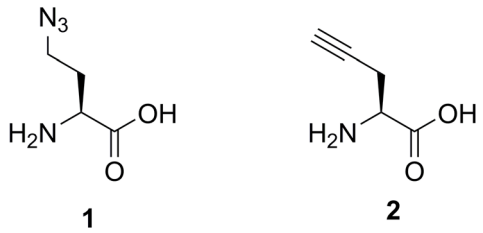

Figure 1. *Structures of Aha (**1**), Pg (**2**).*

To test MHC-I binding and to establish the constraints of performing bioorthogonal ligations within the MHC-I complex, a library of 16 bioorthogonal analogues of the major epitope peptide spanning residues 257-264 of the model antigen ovalbumin ($OVA_{257-264}$; SIINFEKL, Figure 2A) modified with either Aha or Pg at each of the positions within the epitope (P1-P8) was synthesized (Table S1). The binding of these 16 bioorthogonal peptides to the MHC-I molecule H2-K^b was compared against the affinity of the parent epitope, SIINFEKL. Binding was measured using the TAP-deficient RMA-S cell line, which expresses a large fraction of its 10^5 MHC-I molecules with low affinity peptides, when incubated at 26 °C[12]. These low affinity peptides rapidly dissociate when the temperature is raised to 37 °C, resulting in the internalization and degradation of the empty MHC-I complexes. These can, however, be stabilized by co-incubation with a high affinity peptide. Quantification of MHC-I at the cell surface with an anti MHC-I-antibody after incubation at 37 °C for 4 hours thus provides an indirect quantification of MHC-I binding affinity of a particular peptide.
This assay revealed that Aha-substitutions were tolerated in terms of H2-K^b binding at all positions, except the primary anchor residue Phe-5[13] (Figure 2B). Even modifications of P8 and the secondary anchor residues (P2 and P3) were well-tolerated[14]. Pg substitutions in SIINFEKL were tolerated less broadly[15], but still non-anchor positions could be substituted without loss of affinity (Figure 2B)[16].

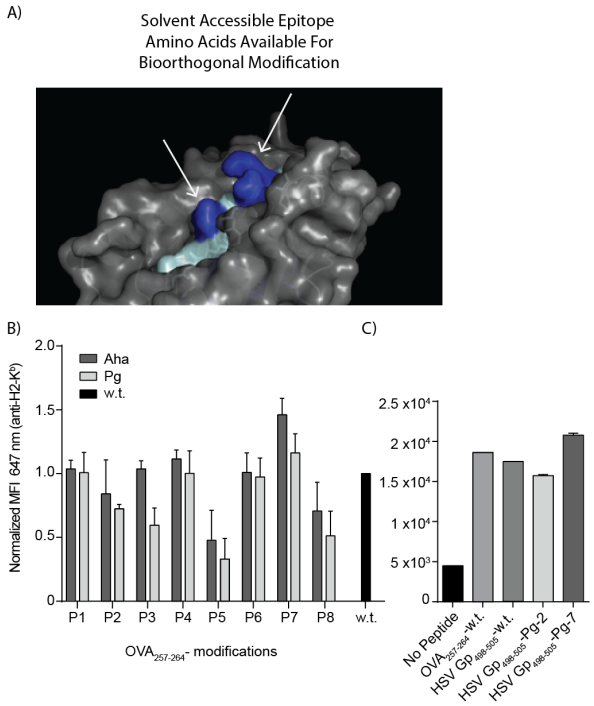

Figure 2. ***Bioorthogonal Antigens****. A) Crystal structure of epitopes within MHC-I complexes allow the prediction of solvent accessible residues available for bioorthogonal modification. Here OVA$_{257-264}$ in H2-K^b with solvent accessible positions 4 and 7 highlighted in blue. B) H2-K^b-rescue by bioorthogonal analogues of SIINFEKL: peptides were exogenously loaded on RMA-S with 1 µM of the indicated bioorthogonal rescue peptides at 37 °C for 4h to allow affinity- dependent stabilization of MHC-I. Positions 1, 4, 6, and 7 can be modified with both azides and alkynes without affecting MHC-I binding affinity and additionally positions 2, 3 and 8 also tolerated azide substitutions. Data obtained from experiments were normalized to the corresponding control of each sample, where the control values were set to equal 1 to account for batch-to-batch variation of MHC-expression on RMA-S cells. All error bars represent the SD of the mean from 3 independent experiments. C) MHC-I stabilization on RMA-S cells of the non-ligatable and ligatable variants of HSV-Gp$_{498-505}$ modified with Pg at the indicated positions: binding of these epitopes is similar to that of the wildtype epitope.*

None of the modified antigens were recognized by the SIINFEKL cognate T cell clone B3Z except for Pg-8 (Figure 3). Binding of the TCR-like antibody that is specific for the peptide SIINFEKL in complex with H2-K^b (antibody 25-D1.16[3]) was observed and found to be in alignment with the known contact sites from the crystal structure of the complex[17]: modifications of P1-P4 (known not to interact with the antibody) were tolerated, whereas modifications of the antibody contact positions P5-P8 abolished 25-D1.16-binding (Figure 4). This discrepancy between B3Z and 25-D1.16 binding highlights the difference in fine specificity between antibody and TCR[17].

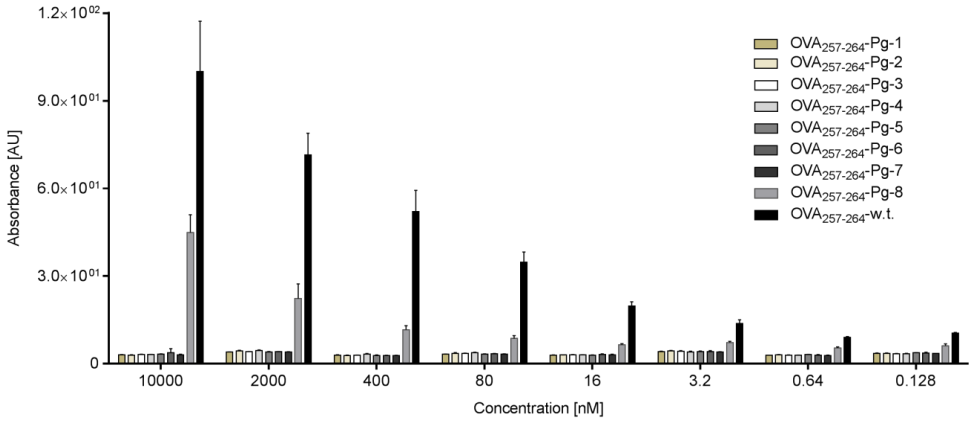

Figure 3. *Reactivity of biorthogonal antigens with the SIINFEKL-specific T cell clone B3Z in T cell assay of Pg-modified SIINFEKL. Peptides were serially diluted 1:5 from 10 µM and incubated with B3Z using standard conditions[1]. Pg-modified SIINFEKL on the anchor position P8 showed a T cell response, but no other position did.*

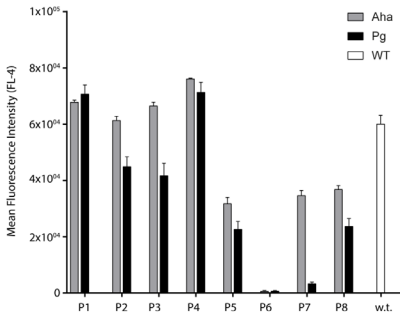

Figure 4. *Binding of complex-specific antibody 25-D1.16 to H-2K^b-bound SIINFEKL analogues (1µM) on RMA-S cells. Modifications of P1-P4 were tolerated, whereas modifications of the antibody contact positions P5-P8 abolished 25-D1.16-binding.*

Optimizing on-surface ligation chemistry

Having shown that positions 1, 4, 6 and 7 can be substituted to Aha and Pg without loss of affinity for H2-K^b, it was next determined whether the bioorthogonal epitopes could be ligated when bound to MHC-I. The suitability of the available azide- and alkyne-reactive bioorthogonal ligation reaction chemistries[7] was tested by comparing the reactivity of unmodified SIINFEKL and the epitopes modified with either azides or alkynes at the solvent-accessible position P7. First, RMA-S cells were pulsed with the different peptides, then ligated to complementary bioorthogonal fluorophores under various conditions and analyzed by flow cytometry for the increase in mean fluorescence intensity upon ligation. In these experiments, none of the attempted modifications of azide-containing epitopes, such as the strain-promoted azide-alkyne cycloaddition reactions (SPAAC; Figure 5), Staudinger ligations and copper(I)-catalyzed Huisgen cycloaddition-reactions (ccHc; Figure 5) gave statistically significant signal-to-noise ratios using the Alexa Fluors.

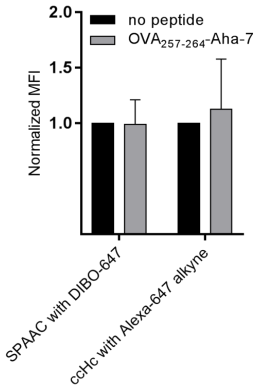

Figure 5. *Normalized mean fluorescence intensity (MFI) in FL-4 channel (647 nm) of the strain-promoted azide-alkyne cycloaddition (SPAAC) with Alexa Fluor-647 DIBO alkyne (DIBO-647) and copper(I)-catalyzed azide-alkyne Huisgen cycloaddition (ccHc) with Alexa Fluor-647-alkyne. Both reactions were performed with $OVA_{257-264}$-Aha-7 and no peptide as control. Data obtained from experiments were normalized to the corresponding control of each sample, where the control equals 1. All error bars represent the SD of the mean from at least 2 independent experiments.*

It was not until the fluorogenic azide-reactive CalFluor-488 was reported[18] and applied during these experiments that significant signal-to-noise ratios were obtained. CF-488 is an alkyne reactive fluorophore that has two properties favorable for these experiments, namely a fluorescence quantum yield that increases of 250-fold upon ccHc-ligation and a zwitterionic head group that likely minimizes cell permeability and a-specific binding (**3**, Figure 6A). One downside of this fluorophore is that the fluorophore core is fluorescein-based, which renders it susceptible to quenching upon prolonged exposure to laser-light and makes it less stable to some conditions found in the cell[19]. This makes it less suitable for microscopy, but readily combined with flow cytometry.

The switch to **3**, in combination with a modified ccHc-reaction protocol in which the cells were first fixed mildly (0.5% paraformaldehyde in PBS) and extensively blocked with 1% BSA and 1% w/v fish gelatin before and after the click-reaction proved optimal to imaging these rare on-cell events. (Figure 6B/D, Figure S1). This did mean that bioorthogonal antigens carrying alkynes in their epitopes were required as the azide-based CalFluors are exclusively alkyne reactive.

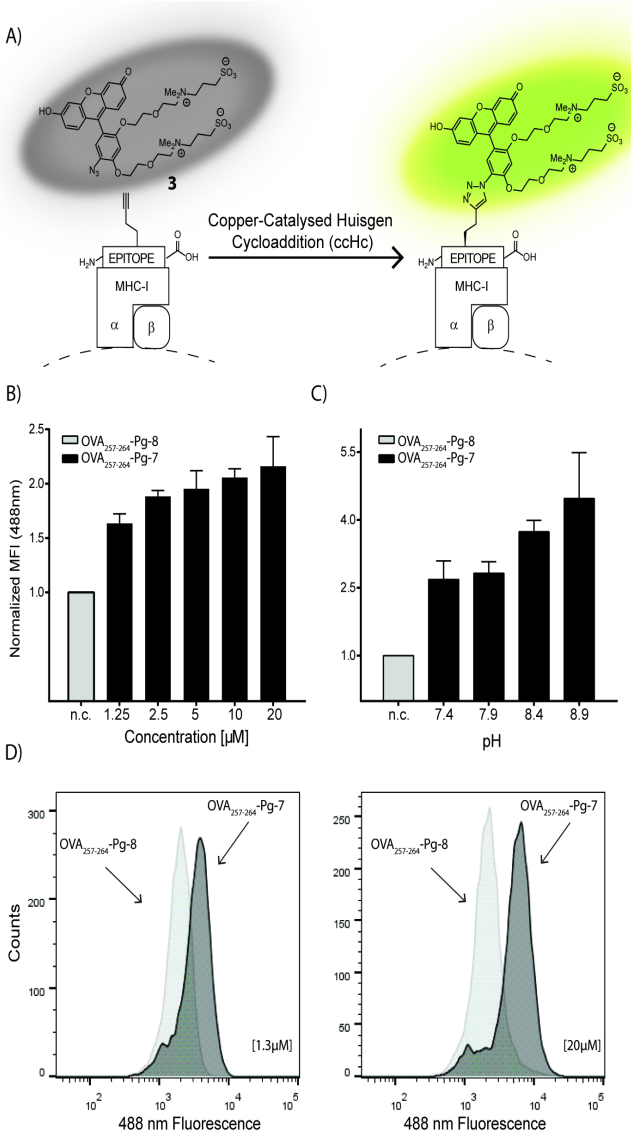

Figure 6. ***Bioorthogonal Ligation Strategy*** *A) MHC-I loaded bioorthogonal epitopes can be modified using the fluorogenic CalFluor-488 dye after MHC-I loading. B) Serial dilution of a solvent accessible $OVA_{257-264}$ -Pg-7 analogue compared to an inaccessible bioorthogonal modification Pg-8 highlights the importance of solvent accessibility in the ligation reaction. C) pH dependence of the CalFluor-ligations: after incubation with 10 μM of epitope peptide and ligation at different pH-values, a dependence of ligation on pH was observed. D) Histograms comparing P7 vs. P8 labeling at 1,3 μM and 20 μM. Data from both experiments were again normalized to the corresponding control of each samples, where the control equals 1. All error bars represent the SD of the mean from 2 independent experiments. n.c.- normalized control.*

The ligation reaction showed a strong dependence on solvent accessibility of the amino acid side chain as determined from the reported crystal structure of $OVA_{257-264}$ presented on H2-$K^{b[20]}$: $OVA_{257-264}$-Pg-8 (of which the Pg-sidechain likely resides in a hydrophobic pocket; Figure 8A) showed no labeling even at very high peptide

concentrations (up to 20 µM). This contrasts with $OVA_{257-264}$-Pg-7, which carries the bioorthogonal sidechain in a solvent exposed area. This epitope showed concentration dependent ligation efficiency (Figure 6B). This supports the hypothesis that the bioorthogonal peptides indeed react whilst bound to H2-K^b, rather than come out of the binding groove, react, and reenter the binding groove. The reaction also showed an increase in reactivity with an increase in pH (Figure 6C), likely due to the reported increased stability of CalFluor at higher pH-values[18].

To assess whether fixation conditions used for the ccHc permeabilized the cells, resulting in labeling of intracellular pMHC-complexes undergoing recycling[21], the modification reaction on unfixed live cells was executed. Using short reaction times, similar labeling for live cell and fixed cell labeling was obtained, suggesting that the contribution of intracellular labeling of recycling pMHC-complexes does not contribute to the overall signal observed in these experiments (Figure7).

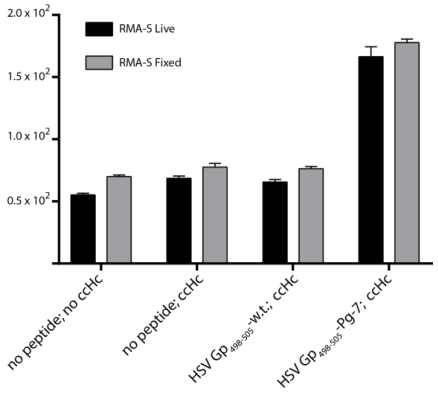

Figure 7. *Comparison of ccHc conditions on cells fixed with 0.5% PFA to ccHc reaction performed on live cells (for these reactions the reaction time was reduced to 15 minutes to prevent permeabilization due to cell death). Cells were loaded with HSV $Gp_{498-505}$-Pg-7 (10 µM) and HSV $Gp_{498-505}$-w.t. (10 µM) and either fixed before ccHc, or used under live cell ccHc-conditions. Assay was set up in triplicate with all error bars correspond to SD of the mean.*

With these optimized ligation conditions in hand, a positional scan of ccHc-reactivity of all positions in $OVA_{257-264}$ on RMA-S was performed and, again quantified by flow cytometry (Figure 8B). These experiments showed a strong correlation of reactivity with solvent-accessibility (as estimated from the reported crystal structure[14]; Figure 8): solvent-accessible[22] positions P4, and P7 showed significant signal-to-noise ratios, whereas P1, P2, P3, P5 and P8 showed no signal over background.

Application to other H2-K^b-binding epitopes

To determine whether the above strategy was restricted only to SIINFEKL variants, or whether other H2-K^b-binding epitopes could also be ligated, the focus went on epitopes for which crystal structures are known and found. The $nucleoprotein_{52-59}$ epitope from the vesicular stomatitis virus (RGYVYQGL)[13, 23] also showed significant labeling when modified at the solvent-accessible residues P4 and P7 (Figure 8C). A second disease-relevant viral epitope, Herpes simplex virus (HSV) glycoprotein $B_{498-505}$ (HSV-$Gp_{498-505}$)[24] also showed reactivity in line with the crystal structure: solvent accessible P4 and P7 could be ligated and solvent inaccessible P2 could not (Figure 9A/D). MHC-affinity of these peptides was identical to the w.t.-HSV-epitope and to SIINFEKL (Figure 2C).

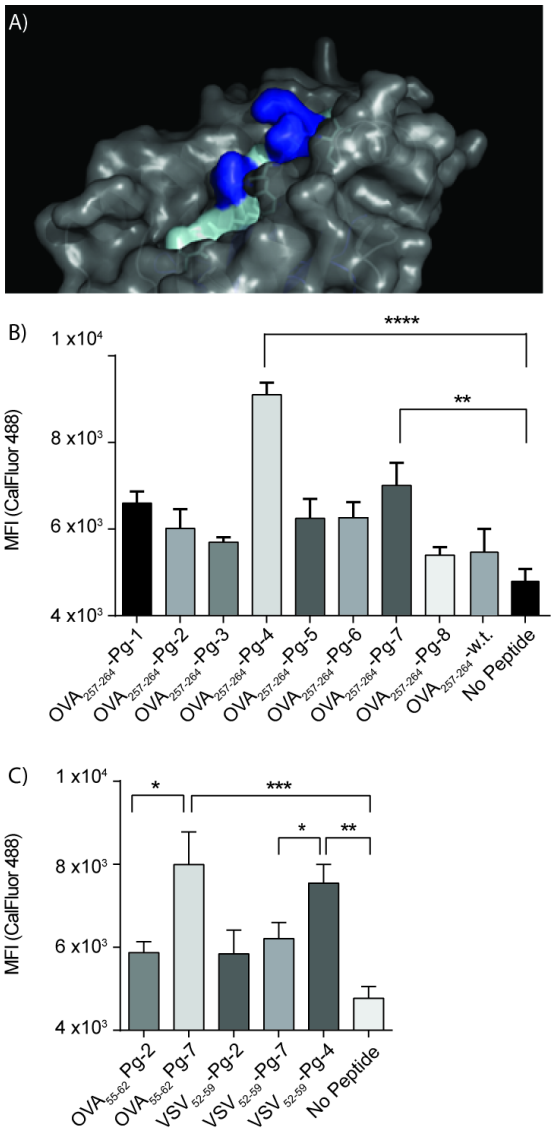

Figure 8. ***Bioorthogonal modification of peptide-MHC-I complexes***. *A) Crystal structure of $OVA_{257-264}$ in H2-K^b with solvent accessible positions 4 and 7 highlighted in dark blue and solvent inaccessible positions in light blue. B) Bioorthogonal ligation of each of the positions in the model antigen SIINFEKL substituted with Pg using CalFluor-488[18]. Solvent accessible positions P4 and P7 gave significant ligations. Solvent inaccessible residues cannot be modified. C) Other epitopes that bind H-2K^b and can be ligated in a ccHc-reaction in solvent accessible positions: P7-position of a second H2-K^b-binding ovalbumin, for which no TCR-reagents are available, OVA_{55-62}, and P4 and P7 position of VSV_{52-59} after incubation of RMA-S with 10 μM of the bioorthogonal epitopes. Assays were set up in triplicate with $^*p \leq 0.05$, $^{**}p \leq 0.01$, $^{***}p \leq 0.001$ and $^{****}p \leq 0.0001$. All error bars correspond to SD of the mean.*

Finally, it was determined whether the approach could be used to determine MHC-loading of epitopes for which no TCR- or antibody reagents exist. Therefore, another reported H2-K^b binding peptides from OVA, for which no T-cell reagents have been reported, despite a reported affinity[22] for H2-K^b haplotype MHC-I[25], namely OVA_{55-62}

was evaluated. This peptide too showed ccHc-reactivity for the predicted solvent accessible modification Pg-7 and not for Pg-2 (Figure 8C).

Due to its robust MHC-I binding, relevance in the immune response against HSV, and robust bioorthogonal labeling, the Pg-7-modified variant of HSV-$GpB_{498-505}$ epitope was explored by performing a serial dilution of HSV-$GpB_{498-505}$-P7 on RMA-S (Figure 9B). A detectable signal over background was still obtained after incubation with 19 nM peptide, which is similar to the sensitivity of detection that can be obtained with a TCR-like antibody[3] highlighting the power of this research tool for the study of antigen presentation.

However, the sensitivity still does not approach that of T cells. In order for this to become a suitable complementary technique to T cell based reagents this sensitivity should improve to the pM-range at which T cells can detect their cognate peptide antigen.

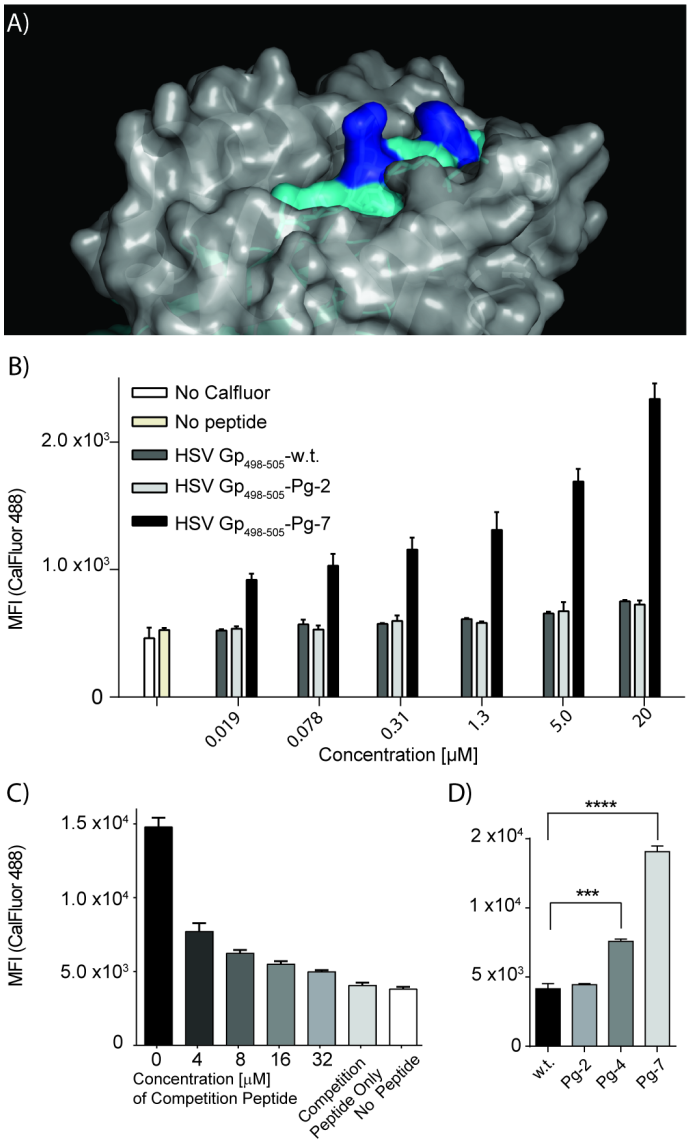

Figure 9. ***Exploration of the Herpes virus glycoprotein$_{498\text{-}505}$ epitope for bioorthogonal ligation***. *A) Crystal structure of HSV-Gp$_{498\text{-}505}$ with solvent accessible positions P4 and P7 shown in blue[23]. B) Serial dilution of bioorthogonal peptides on RMA-S. Assays were set up in triplicate with $^{***}p \leq 0.001$ and $^{****}p \leq 0.0001$. All error bars correspond to SD of the mean. C) Competition with unlabeled H2-K^b-binding epitope showed that the signal resulting from bioorthogonal ligation is reduced upon increasing concentration of competing peptide. As competing peptide w.t. HSV Gp$_{498\text{-}505}$ was used. D) Bioorthogonal modification of the Herpes Virus Gp$_{498\text{-}505}$ Epitope: position 7 is most readily reacted in a ligation reaction; Figure S2 shows the raw data for this figure.*

To assess the application of the approach to imaging bioorthogonal epitope peptides, the labeling on non-TAP deficient cell lines was attempted. The growth factor dependent dendritic cell line D1[26] was used as these cells have active TAP-transporter complexes (unlike RMA-S cells); they are loaded with higher affinity

peptides, making the exchange of exogenous peptides proceed with lower efficiency. Despite this limitation, the exchange and ligation of bioorthogonal peptides on these cells could still be detected, albeit with lower signal-to-noise ratios (Figure 10). As for the RMA-S experiments, only peptides modified in solvent-accessible positions once bound to MHC-I showed effective bioorthogonal ligation.

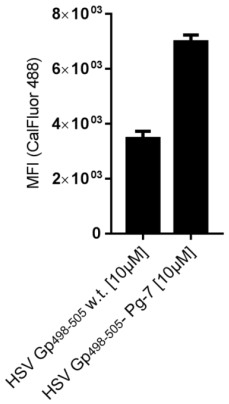

Figure 10. *ccHc of HSV $Gp_{498-505}$-loaded D1-cells. Ligation characteristics were the same as for RMA-S labeling, with HSV $Gp_{498-505}$ w.t. control peptide showing minimal labeling, where the solvent exposed P7 labeled strongly. Data obtained from experiments were normalized to the corresponding control of each samples, where the control equals 1. All error bars represent the SD of the mean from 2 independent experiments.*

Reactivity of MHC-bound epitopes

To determine what percentage saturation of the 10^5 MHC-Is[27] could be detected, a competition experiment was performed: bioorthogonal peptides were co-incubated with increasing concentrations of unlabeled control peptides (Figure 9C). Bioorthogonal ligation yields indeed showed an inverse correlation with concentration of the unlabeled competition peptide. However, even at a concentration of competing peptide of 32 μM, detectable signal could be observed. Presuming equal affinity of the two peptides for MHC-I, this means that the peptide could be detected at <10% saturation level within the H2-K^b peptide binding groove, suggesting this approach could be used to image 10^4 molecules per cell.

Taken together, the here presented data suggest that bioorthogonal epitopes can bind and be quantified within MHC-complexes at physiologically relevant concentrations and may serve as a useful tool for studying pMHC-I biology on the surface of cells. The requirement is that non-anchor residues in solvent-accessible positions are modified, which results in peptides capable of both binding MHC-I and of being ligated using a fluorogenic ccHc-variant.

Super-resolution approaches to visualize bioorthogonal epitopes

A major limitation that was observed for the above approach was that – using the concentrations required to obtain a signal in conventional confocal microscopy – background fluorescence was too high to image peptide appearance. Recent years have seen a surge in the development of diffraction-limit breaking microscopy techniques which use a plethora of elegant physical tricks to break the diffraction barrier[28] to obtain an image at high resolution and a nanometer localization precision of a single fluorescent molecule[29]. One of those techniques is a stochastic optical reconstruction microscopy (STORM)[30] with a resolution of ~20 nm which is

an order of magnitude below the diffraction limit[31]. The enhanced resolution is achieved through the precise localization of single fluorescent molecules that can be switch on between a fluorescent and a dark state that allow for separating in time the otherwise spatially overlapping light diffractions of the fluorescent molecules[32]. By repeatedly switching 'on' and 'off' the fluorescent molecules and overlaying the resulting localizations, a super-resolution image can be reconstructed (Figure 11)[33].

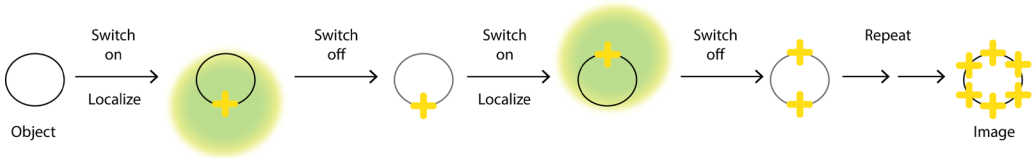

Figure 11. *The principle of stochastic optical reconstruction microscopy (STORM). STORM exploits fluorescent dyes that can be switch between fluorescent and dark states which enables for determining their positions with high precision in every snapshot. The process is repeated until all the fluorescent dyes are exhausted due to photo-bleaching. The positions of localized dyes are indicated with yellow crosses. The final super-resolution image is reconstructed from the all measured positions of the fluorescent dyes (Adapted from Dempsey et. al., Nat. Meth. (2011)).*

It was thus postulated that STORM-based methods, could improve the signal to noise ratio to allow the detection of peptides using non-fluorogenic, microscopy compatible fluorophores.

However, as it was already found that even the sulfonated Alexa-dyes gave too much background, an approach applied in correlative light-electron microscopy to enhance signal of low numbers of fluorophores was used to isolate surface-signal from intracellular signal[34]: first all bioorthogonal groups in the cell were modified with a small molecule fluorophore (Alexa Fluor-488) using the ccHc-reaction (giving random intracellular labeling). Then, to selectively image the cell-surface population only of the fluorophore, an anti-Alexa-488 antibody to which cells have not become permeable during fixation and ccHc was added (Figure 12), which in turn could be visualized using Alexa Fluor-647-conjugated protein A (Figure 13). This latter fluorophore has excellent properties for STORM and in this manner, could not only intracellular background be eliminated, but also an enhancement of the cell surface signal be achieved.

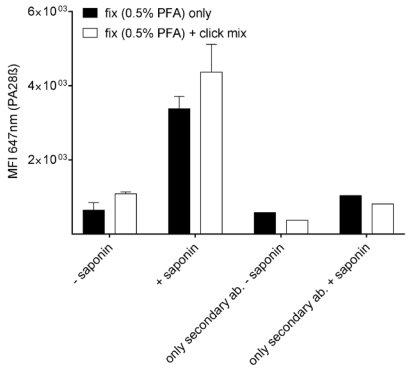

Figure 12. *The ccHc conditions did not permeabilized the D1 cells to an antibody (~150 kDa), which was assessed by quantifying the mean fluorescence intensity of the cytosolic antibody (PA28β) in the presence and absence of the permeabilizing agent – saponin (0.1 %). Assay was set up in triplicate. All error bars correspond to SD of the mean.*

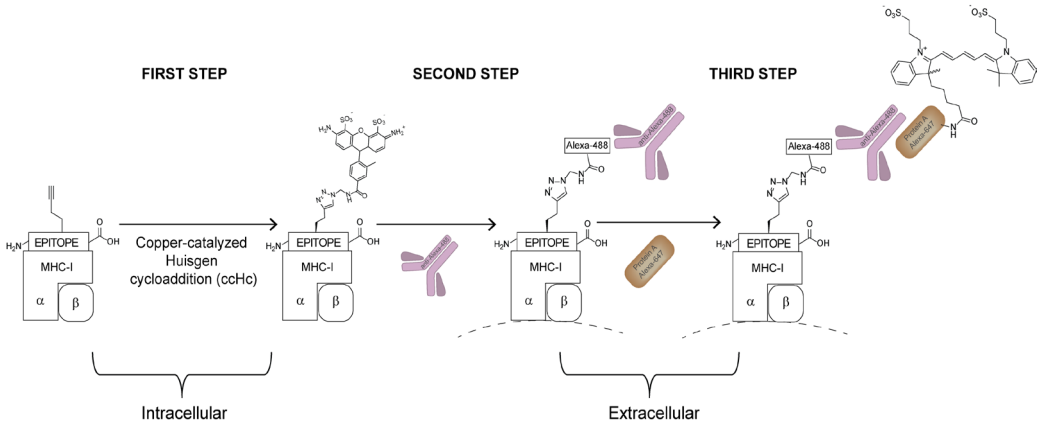

Figure 13. *Schematic overview of the technique that allows for imaging both the intracellular and cell-surface pool of antigen in a single experiment. Bioorthogonal labeling was performed using the Alexa Fluor-488 azide in ccHc reaction followed by anti-Alexa Fluor-488 antibody binding step and finally by visualizing the antibody with Alexa Fluor-647-conjugated protein A.*

To assess whether this three-step labeling could work, the minimal epitopes that showed most robust labeling in the above described CalFluor-FACS-experiments were used for the preliminary STORM imaging experiments. For that the OVA model antigens modified with Propargylglycine (Pg) at position 4 and 7 within the epitope (SII**Pg**FEKL and SIINFE**Pg**L) and the second viral epitope, Herpes simplex virus (HSV) modified with Pg at position 7 (SSIEFA**Pg**L) were chosen (Table S1). As an initial test to determine whether these minimal epitope peptides could be labeled and selectively imaged at the cell surface, the $OVA_{257-264}$-Pg-4, –Pg-7 and HSV $Gp_{498-505}$-Pg-7 (as well as their non-bioorthogonal controls) were incubated with the C57Bl/6-derived dendritic like cell line DC2.4[35] at various concentrations for ~1.5h at 37°C followed by wash, fixation and exposure to the ccHc labeling using Alexa Fluor-488, followed by anti-Alexa Fluor-488 antibody and finally the Alexa Fluor-647 conjugated protein A. The cells were first imaged on super resolution microscopy using an epi-fluorescence illumination phase (without using quenching-blinking) with a white-light LASER. These images revealed that using this three- step labeling approach, the HSV $Gp_{498-505}$-Pg-7 peptide could be labeled and imaged at the cell surface of the DC2.4 cells with a substantial signal to noise ratio (Figure 14; no significance could be determined as only one biological replicate was performed).

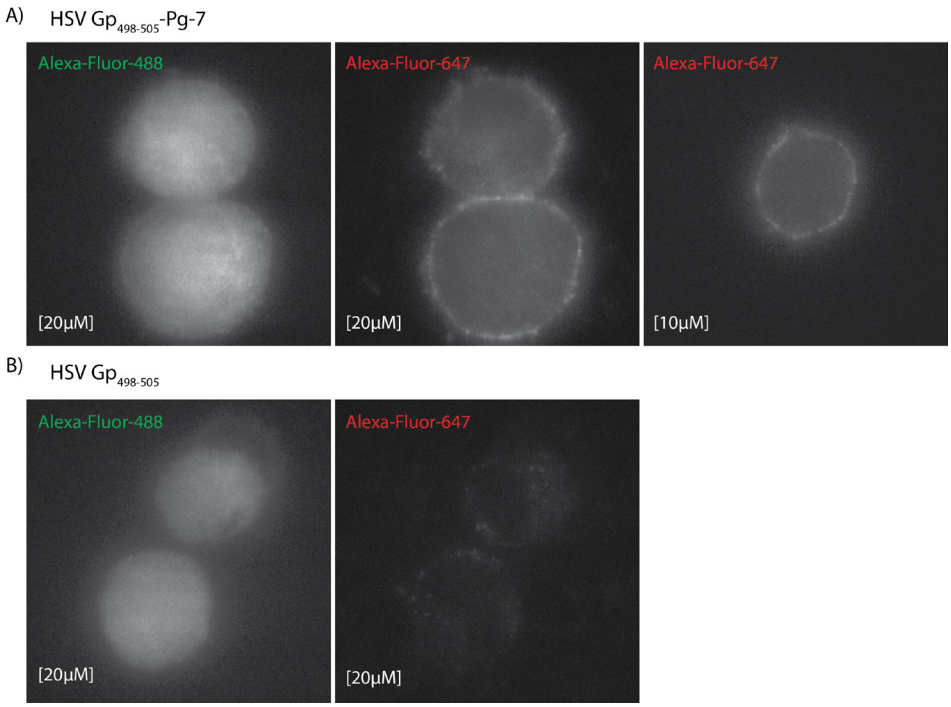

Figure 14. *Epi-fluorescence illumination phase with white-light microscopy images of A) HSV $Gp_{498-505}$-Pg-7 at 20μM as well as at 10μM provided a substantial signal to noise ratio as compared to its non-bioorthogonal control B) DC2.4 were incubated with the indicated peptides for 1.5h followed by wash with medium complete, fixation and exposure to the three- step labeling as described above.*

Interestingly, the fluorescence signal obtained from $OVA_{257-264}$-Pg-4 and –Pg-7 was much weaker than that of HSV $Gp_{498-505}$-Pg-7 (Figure S3). The origin of this lack of signal remains unknown, but could be the result of less efficient ccHc-labelling of the OVA-peptides (as also observed in the FACS-experiments) perhaps due to diminished accessibility of the side-chains. Alternatively, it can be postulated that the HSV $Gp_{498-505}$-Pg-7 has stronger a-specific cell surface binding, resulting in an inflated signal. This is, however, something that has to be further explored in future experiments.

The successful trial of imaging $Gp_{498-505}$-Pg-7 peptide led to the execution of the super resolution microscopy of the peptide and its non-bioorthogonal control using the blinking properties of Alexa Fluor-647 (Figure 15).

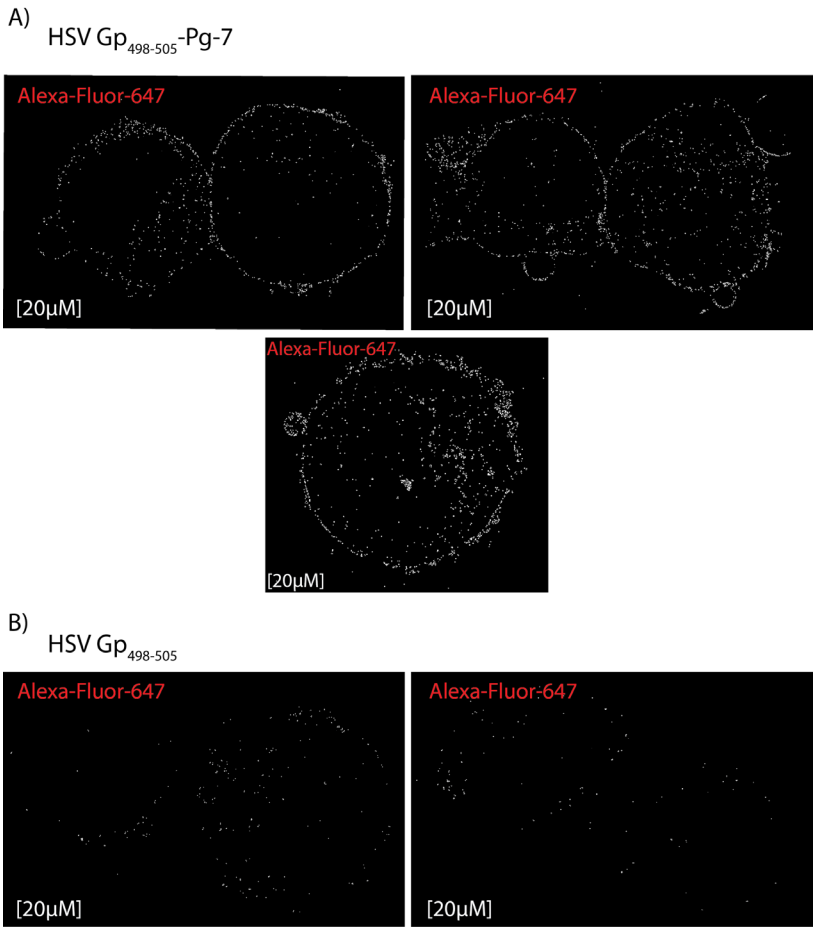

Figure 15. *STORM imaging of HSV $Gp_{498-505}$-Pg-7 allowed for visualization of the peptide at the cell surface. DC2.4 were incubated with HSV $Gp_{498-505}$-Pg-7 and w.t. (20μM) for 1.5h followed by wash with medium complete, fixation and exposure to the three- step labeling as described above.*

These preliminary results indicate that STORM-imaging of epitopes can in potential result in the localization of individual fluorophores on the cell surface. However, first the lack of broad reactivity in this assay of other epitopes must be explored, as well as the localization within the MHC-I complex confirmed.

3.3 Conclusion

The bioorthogonal ligation using fluorogenic Calfluor-488 in combination with a Cu(I)-catalyzed Huisgen cycloaddition reaction allowed for the bioorthogonal epitopes to be quantified within MHC-complexes at physiologically relevant concentrations. This approach can make the bioorthogonal epitopes a useful addition to the antigen presentation toolkit as quantification of antigenic peptides for which no T cell (or other) reagents are available, such as the H2-K^b-binding peptide OVA_{55-62} reported herein. The broad scope of bioorthogonal chemistry[36] and the breadth of tools

available to incorporate minimal bioorthogonal functionalities into peptides, proteins[37] from both prokaryotic expression systems[38], as well as eukaryotic ones[39], and whole cells[9a] including various pathogens[40] suggests that this approach could potentially extend to study the rates at which antigen presenting cells process exogenous antigens for the activation of CTLs – so-called antigen cross-priming. The stability of bioorthogonal groups would be very beneficial here, as antigens encounter some of the harshest conditions known in the human body in the endo-lysosomes of antigen presenting cells, with both strongly oxidizing[41] and reducing conditions found during cross-presentation[42].

The preliminary results of the STORM imaging of bioorthogonal epitopes using the three-step labeling revealed a potential to localize and later quantify the epitopes on the cell surface. In the future, this approach can be applied to the synthetic long peptides (SLPs) in order to visualize the intra and extracellular localization of the antigen during antigen cross-presentation.

3.4 Supporting table and figures

Position of Handle	*Peptide Sequence*	*Peptide Name*	*Source*
P1	**Pg**IINFEKL	$OVA_{257-264}$-Pg-1	Ovalbumin (*Gallus gallus*)
P2	S**Pg**INFEKL	$OVA_{257-264}$-Pg-2	Ovalbumin (*Gallus gallus*)
P3	SI**Pg**NFEKL	$OVA_{257-264}$-Pg-3	Ovalbumin (*Gallus gallus*)
P4	SII**Pg**FEKL	$OVA_{257-264}$-Pg-4	Ovalbumin (*Gallus gallus*)
P5	SIIN**Pg**EKL	$OVA_{257-264}$-Pg-5	Ovalbumin (*Gallus gallus*)
P6	SIINF**Pg**KL	$OVA_{257-264}$-Pg-6	Ovalbumin (*Gallus gallus*)
P7	SIINFE**Pg**L	$OVA_{257-264}$-Pg-7	Ovalbumin (*Gallus gallus*)
P8	SIINFEK**Pg**	$OVA_{257-264}$-Pg-8	Ovalbumin (*Gallus gallus*)
P1	**Aha**IINFEKL	$OVA_{257-264}$-Aha-1	Ovalbumin (*Gallus gallus*)
P2	S**Aha**INFEKL	$OVA_{257-264}$-Aha-2	Ovalbumin (*Gallus gallus*)
P3	SI**Aha**NFEKL	$OVA_{257-264}$-Aha-3	Ovalbumin (*Gallus gallus*)
P4	SII**Aha**FEKL	$OVA_{257-264}$-Aha-4	Ovalbumin (*Gallus gallus*)
P5	SIIN**Aha**EKL	$OVA_{257-264}$-Aha-5	Ovalbumin (*Gallus gallus*)
P6	SIINF**Aha**KL	$OVA_{257-264}$-Aha-6	Ovalbumin (*Gallus gallus*)
P7	SIINFE**Aha**L	$OVA_{257-264}$-Aha-7	Ovalbumin (*Gallus gallus*)
P8	SIINFEK**Aha**	$OVA_{257-264}$-Aha-8	Ovalbumin (*Gallus gallus*)
P2	K**Pg**VRFDKL	OVA_{55-62}-Pg-2	Ovalbumin (*Gallus gallus*)
P7	KVVRFD**Pg**L	OVA_{55-62}-Pg-7	Ovalbumin (*Gallus gallus*)
P2	R**Pg**YVYQGL	VSV_{52-59}-Pg2	Vesicular Stomatitis Virus Nucleoprotein
P4	RGY**Pg**GQGL	VSV_{52-59}-Pg4	Vesicular Stomatitis Virus Nucleoprotein
P7	RGYVYQ**Pg**L	VSV_{52-59}-Pg7	Vesicular Stomatitis Virus Nucleoprotein
P2	S**Pg**IEFARL	HSV $Gp_{498-505}$-Pg-2	Herpes Simplex Virus GpB
P4	SSI**Pg**FARL	HSV $Gp_{498-505}$-Pg-4	Herpes Simplex Virus GpB
P7	SSIEFA**Pg**L	HSV $Gp_{498-505}$-Pg-7	Herpes Simplex Virus GpB

Table S1. *Overview of all modified epitope peptides used in this study.*

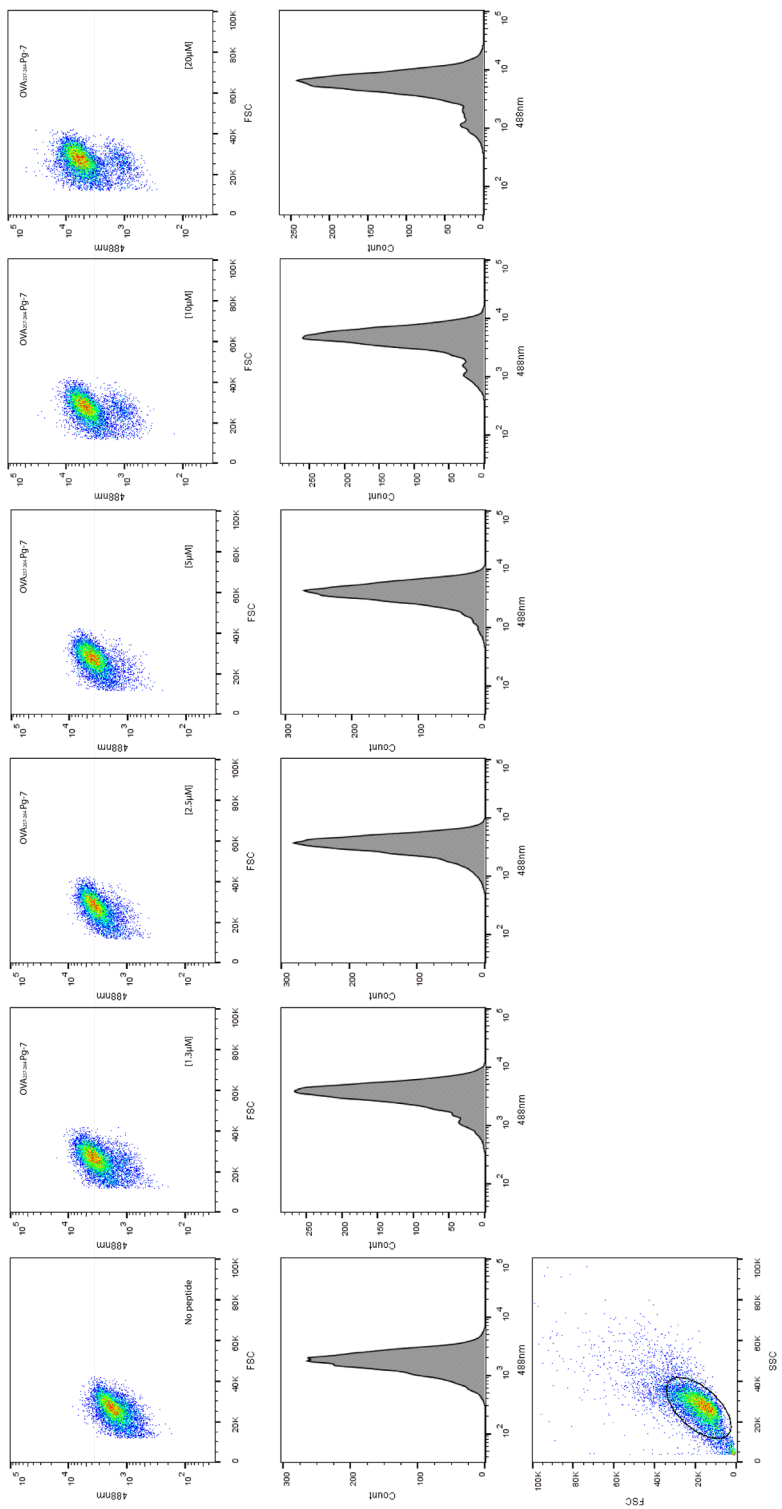
No peptide
[1.3μM]
[2.5μM]
[5μM]
[10μM]
[20μM]
FSC
SSC
488nm
Count

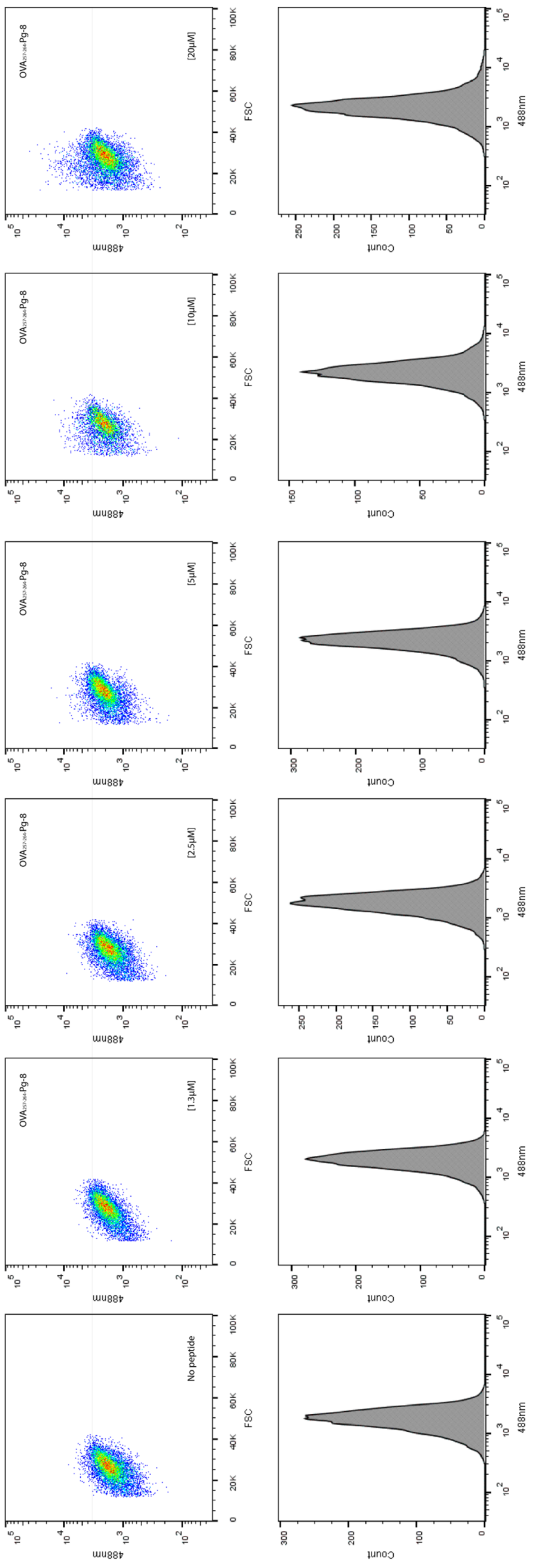
No peptide
[1.3μM]
[2.5μM]
[5μM]
[10μM]
[20μM]
488nm
FSC
Count

Figure S1: *(Previous two pages); Flow cytometry data underpinning Figure 6B: Fluorescence intensity in the FL-1-channel (488 nm) on gated cells was plotted for different peptide concentrations. A) FACS plots of P7-modifications. B) FACS plots of P8-modifications.*

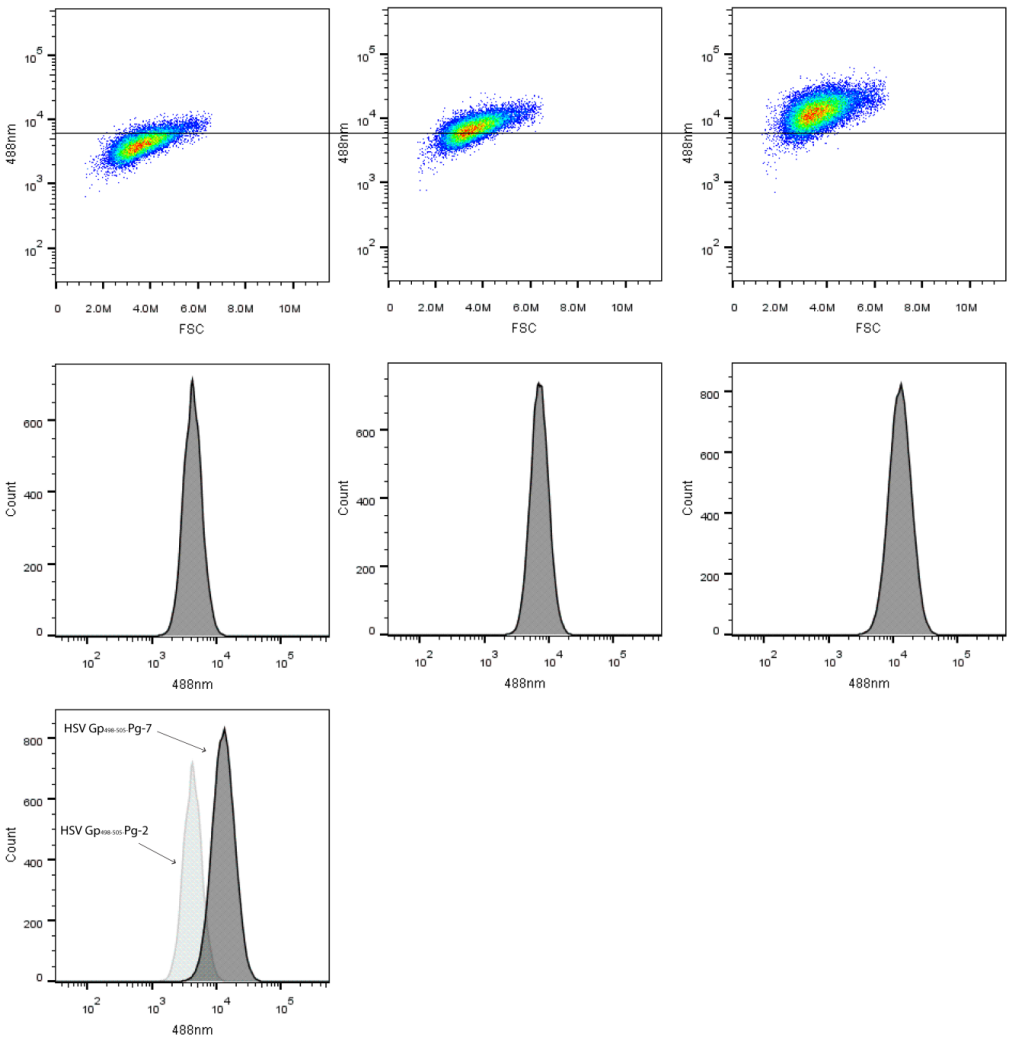

Figure S2. *FACS data underpinning Figure 9D. FACS plots and corresponding histograms of HSV $Gp_{498-505}$-Pg-2 (left panel), -Pg-4 (middle panel) and -Pg-7 (right panel).*

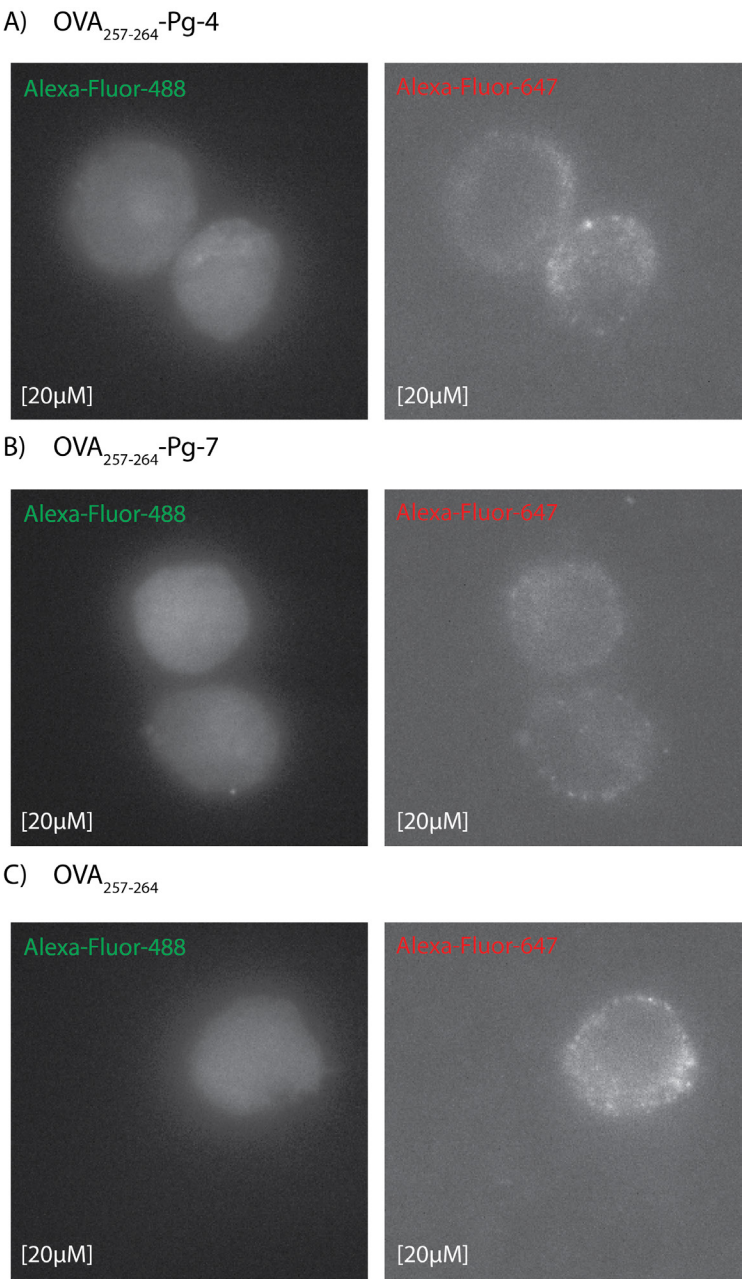

Figure S3. *Epi-fluorescence illumination phase with white-light microscopy images of A) $OVA_{257-264}$-Pg-4 at 20µM as well as B) $OVA_{257-264}$-Pg-7 at 20µM did not show any signal to noise ratio as compared to their non-bioorthogonal control. C) DC2.4 were incubated with the indicated peptides for 1h followed by wash with medium complete, fixation and exposure to the three- step labeling as described above.*

3.5 Experimental section

Reagents:
Azidohomoalanine and Propargylglycine-Fmoc were purchased from Anaspec. Tris(3-hydroxypropyl-triazolylmethylamine) (THPTA) was purchased from Sigma-Aldrich, as were all other reagents at the highest available grade. Mouse Anti-Mouse H-2K^b (B8-24-3 clone) was made in-house. 25-D1.16-APC conjugated was purchased from eBioscience (Cat. #: 12-5743-81) (APC conjugated in-house). Secondary antibody (Goat anti-Mouse IgG conjugated to Alexa Fluor-647 (catalogue number: A-21235) was purchased from Thermo Fisher Scientific. All solvents were purchased from Biosolve Ltd. Phosphate buffered saline (PBS) is 5 mM KH_2PO_4, 15 mM Na_2HPO_4, 150 mM NaCl, pH 7.4. Alexa Fluor-488 azide (catalogue number: A10266), AlexaFluor-488 polyclonal antibody (catalogue number: A-11094) and Alexa Fluor-647-conjugated protein A (catalogue number: P21462) as well as donkey anti-goat IgG (H+L) secondary antibody, Alexa Fluor-647 (catalogue number: A-21447) were purchased from Thermo Fisher Scientific. PA28β antibody (catalogue number: SC-23642) was purchased from Santa Cruz biotechnology.

Peptide synthesis:
All peptides were synthesized using standard Fmoc Solid Support Chemistry and purified using high performance liquid chromatography (Prep column Gemini C18 110A 150x21.20 5µm) using 15 to 45 % gradient (A: 0.1% TFA in MilliQ H2O, B: ACN). LC-MS measurements were done on an API 3000 Alltech 3300 with a Grace Vydac 214TP 4,6 mm x 50 mm C4 column and analyzed by electrospray LC-MS analysis on a PE SCIEX: API 3000 LC/MS/MS system using a Gemini 3u C18 110A analytical column (5µ particle size, flow: 1.0 mL/min), on which the absorbance was also measured at 214 and 254 nm. Solvent system for LC-MS: A: 100% water, B: 100% acetonitrile, C: 1% TFA (aq).

Cell culture:
The D1 cell line, a long-term growth factor-dependent immature myeloid (CD11b$^+$, CD8α$^-$) DC line of splenic origin, derived from a female C57BL/6 mouse which was provided by M. Camps (Leiden University Medical Center) and was cultured as described previously[43].
The DC2.4 cell line, an adherent C57BL/6 bone marrow derived DC line was kindly provided by Dr. Kenneth Rock (University of Massachusetts Medical School) and cultured as described previously[35, 44].

CalFluor-488 synthesis:
CalFluor-488 was synthesized as described previously[18].

RMA-S MHC I-binding and stability assays:
RMA-S assays were essentially performed as described previously[12, 45]. Briefly, RMA-S cells were grown and passaged at 37 °C, 5% CO_2 in RPMI-1440 augmented with 10% FCS and antibiotics. Prior to the experiment, the incubation temperature was lowered to 26 °C for 48 hours (10^6 cells/mL) to ensure metastable MHC-I surface expression. For affinity tests, cells were incubated with rescue peptides in serum free medium at the indicated concentrations for 4 hours and washed in protein blocking agent (PBA: 5% BSA in PBS + 0.1% w/v NaN_3). For MHC-I peptide complex stability assays, 26°C RMA-S cells were pulsed for 1 hour with respective peptides at the indicated concentrations, and washed thoroughly in ice-cold serum free medium, after which they were placed back at 37 °C and chased for the indicated time.

After each timepoint, cells were fixated in 4% fixation buffer (Cat #420801, Biolegend) for 30 minutes. After this time, the cells were washed with PBA. Both assays were subsequently stained with anti-Mouse-H-2K^b (400 ng/mL; >60 µL/well) in PBA for 30 minutes on ice, prior to washing with PBA twice. Secondary antibody (Goat anti-Mouse IgG conjugated to AlexaFluor-647; 5 µg/mL) was added and the cells were again incubated on ice for 30 minutes prior to washing twice with PBA before analysis. Analysis was performed on a BD Accuri™ C6 Plus Flow Cytometer. All flow cytometry data was analyzed using FlowJo v10.1 (Miltenyi Biosciences).

25-D1.16-binding of bioorthogonal epitopes:
RMA-S cells were incubated with a serial dilution of peptides as above. After the 4-hour loading period and blocking, cells were incubated with 25-D1.16-APC conjugated antibody (1.3 µg/mL; >60 µL/well, conjugated in-house)[3] in PBA for 30 minutes on ice, prior to washing with PBA twice. Cells were analyzed by flow cytometry as described above. Fluorescence intensity in the APC-channel was plotted against peptide concentration at 1µM (as in Figure 4).

Bioorthogonal modification reactions on RMA-S cells:
RMA-S cells were grown and as described above for the binding assay and plated in 96-well v-bottom microtiter plate (4x10^5 cells/well) in serum free medium and incubated for ~1h at 37°C with respective peptides at the indicated concentrations. After the incubation, the cells were washed twice in PBS and subsequently fixed for 1 hour at RT in 0.5% PFA in PBS (Cat #420801, Biolegend; diluted 1:8) and washed twice more with PBS. Cells were then exposed to the bioorthogonal labeling mixture (1 mM $CuSO_4$, 10 mM sodium ascorbate, 1 mM THPTA ligand, 10 mM aminoguanidine, 100 mM HEPES, pH 8.4, CalFluor-488 10µM). After 45 minutes at RT, the reaction mixture was aspirated and the cells were blocked with 1% BSA and 1% fish gelatin before being washed twice with PBS prior to analysis by flow cytometry. Assays were set up in triplicate, unless otherwise indicated. The statistical significance of the indicated differences was analyzed by the two-tailed student's t-test with the significance specified using *p* values with $^*p \leq 0.05$, $^{**}p \leq 0.01$, $^{***}p \leq 0.001$ and $^{****}p \leq 0.0001$. All error bars correspond to SD of the mean.

Reactivity of bioorthogonal SIINFEKL peptides in a B3Z T cell assay:
RMA-s cells were grown as described above and plated in 96-well tissue-culture treated microtiter plate (5x10^4 cells/well) and incubated for 1h at 37°C with SIINFEKL modified peptides at the indicated concentrations, followed by a wash with complete IMDM. After the wash, the T cell hybridoma B3Z cells (5x10^4 cells/well) were added. The RMA-S and T cells were co-cultured for 17 h at 37°C. Stimulation of the B3Z hybridoma was measured by a colorimetric assay using CPRG (chlorophenol red-β-D-galactopyranoside) as a substrate as described[46].

Competition assay with unlabeled peptide:
RMA-S cells were grown and treated as described above for the bindings assay, prior to loading. Incubation of RMA-S cells with HSV-Gp$_{498\text{-}505}$-Pg7 epitopes was performed for 4 hours at 4 µM, in presence of increasing amounts of w.t. HSV-Gp$_{498\text{-}505}$ at the indicated concentrations. The amount of peptide in all samples was equalized to 36µM by adding the lacking amount of adenoviral H-2D^b binding epitope of the human Adenovirus 5 E1a protein Ad10$_{234\text{-}243}$[47]. Bioorthogonal ligation was subsequently performed as described above.

Permeability assay:
D1s were collected using 2mM EDTA in PBS, fixed in 0.5% PFA in PBS for 1h at RT and exposed to the click cocktail mix (as described previously but without a fluorophore) for 1h at RT. After the wash, cells were permeabilized with 0.1% saponin in 1% BSA in PBS (control cells were incubated without saponin throughout whole experiment) for ~20min at RT followed by incubation with PA28β antibody (final concentration 2µg/mL) in 0.1% saponin in 1% BSA in PBS for 30min on ice followed by wash and incubation with the donkey anti-goat IgG (H+L) secondary antibody (0.5µg/mL) in 0.1% saponin in 1% BSA in PBS for 30min on ice followed by wash and analysis by Guava EasyCyte™ flow cytometry (Merck Millipore) and using FlowJo v10.1.

The three- step labeling:
The DC2.4 cells were incubated with respective peptides, at the indicated concentrations and times. After the incubation, the cells were washed ones with medium complete and ones with PBS. The cells were fixed by adding 2% PFA in PBS for 20min at RT followed by double wash with PBS. The fixed DC2.4 were then exposed to the bioorthogonal labeling mixture (1 mM $CuSO_4$, 10 mM sodium ascorbate, 1 mM THPTA ligand, 10 mM aminoguanidine, 100 mM HEPES, pH 8.4, Alexa Fluor-488-azide 5µM). After 1h at RT, the reaction mixture was aspirated and the cells were blocked with 1% BSA and 1% fish gelatin before being washed twice with PBS. Next, the cells were incubated with an Alexa Fluor-488 antibody (final concentration 2µg/mL) in 100mM HEPES pH 7.2 supplemented with 1% BSA and 1% fish gelatin for 1h at RT. After the incubation, cells were washed with PBS and blocked with 1% BSA and 1% fish gelatin before being exposed to Alexa Fluor-647-conjugated protein A (final concentration 5µg/mL) for 20min at RT followed by PBS wash step and blocking with 1% BSA and 1% fish gelatin.

Stochastic optical reconstruction microscopy and sample preparation:
After the three- step labeling, the samples were exposed to STORM buffer which is composed of 50 mM HEPES buffer (pH=8.5), 1 M NaCl, an oxygen-scavenging system (0.5 mg mL^{-1} glucose oxidase, 40 µg mL^{-1} catalase, 5 wt % glucose) and 200 mM 2-aminoethanethiol.
STORM images were acquired using a Nikon N-STORM system configured for total internal reflection fluorescence (TIRF) imaging. Excitation inclination was tuned to adjust focus and to maximize the signal-to-noise ratio. Alexa Fluor-647 was excited illuminating the sample with the 647 nm (∼160 mW) laser line built into the microscope. Fluorescence was collected by means of a Nikon 100x, 1.4NA oil immersion objective and passed through a quad-band-pass dichroic filter (97335 Nikon). 20,000 frames were acquired for the 647 channel and 10,000 frames for the 488 channel (WGA-AF561). Images were recorded onto a 256 × 256 pixel region (pixel size 160 nm) of a CMOS camera. STORM images were analyzed with the STORM module of the NIS element Nikon software.[30b]

3.6 References

[1] J. Karttunen, N. Shastri, *Proc Natl Acad Sci U S A* **1991**, *88*, 3972-3976.

[2] aB. Laugel, J. M. Boulter, N. Lissin, A. Vuidepot, Y. Li, E. Gostick, L. E. Crotty, D. C. Douek, J. Hemelaar, D. A. Price, B. K. Jakobsen, A. K. Sewell, *J Biol Chem* **2005**, *280*, 1882-1892; bY. Li, R. Moysey, P. E. Molloy, A.-L. Vuidepot, T. Mahon, E. Baston, S. Dunn, N. Liddy, J. Jacob, B. K. Jakobsen, J. M. Boulter, *Nature Biotechnology* **2005**, *23*, 349-354; cW. F. Hoo, M. J. Lacy, L. K. Denzin, E. W. Voss, Jr., K. D. Hardman, D. M. Kranz, *Proc Natl Acad Sci U S A* **1992**, *89*, 4759-4763; dJ. S. Huston, D. Levinson, M. Mudgett-Hunter, M. S. Tai, J. Novotny, M. N. Margolies, R. J. Ridge, R. E. Bruccoleri, E. Haber, R. Crea, *Proceedings of the National Academy of Sciences of the United States of America* **1988**, *85*, 5879-5883.

[3] A. Porgador, J. W. Yewdell, Y. Deng, J. R. Bennink, R. N. Germain, *Immunity* **1997**, *6*, 715-726.

[4] J. A. Prescher, D. H. Dube, C. R. Bertozzi, *Nature* **2004**, *430*, 873-877.

[5] W. Ma, Y. Zhang, N. Vigneron, V. Stroobant, K. Thielemans, P. van der Bruggen, B. J. Van den Eynde, *J Immunol* **2016**, *196*, 1711-1720.

[6] J. W. Yewdell, E. Reits, J. Neefjes, *Nat Rev Immunol* **2003**, *3*, 952-961.

[7] K. Lang, J. W. Chin, *ACS Chemical Biology* **2014**, *9*, 16-20.

[8] J. B. Pawlak, G. P. Gential, T. J. Ruckwardt, J. S. Bremmers, N. J. Meeuwenoord, F. A. Ossendorp, H. S. Overkleeft, D. V. Filippov, S. I. van Kasteren, *Angew Chem Int Ed Engl* **2015**, *54*, 5628-5631.

[9] aK. L. Kiick, D. A. Tirrell, *Tetrahedron* **2000**, *56*, 9487-9493; bJ. C. M. van Hest, K. L. Kiick, D. A. Tirrell, *Journal of the American Chemical Society* **2000**, *122*, 1282-1288.

[10] aR. Ekkebus, S. I. van Kasteren, Y. Kulathu, A. Scholten, I. Berlin, P. P. Geurink, A. de Jong, S. Goerdayal, J. Neefjes, A. J. Heck, D. Komander, H. Ovaa, *J Am Chem Soc* **2013**, *135*, 2867-2870; bS. Sommer, N. D. Weikart, U. Linne, H. D. Mootz, *Bioorg Med Chem* **2013**, *21*, 2511-2517.

[11] P. P. Geurink, L. M. Prely, G. A. van der Marel, R. Bischoff, H. S. Overkleeft, *Top Curr Chem* **2012**, *324*, 85-113.

[12] H. G. Ljunggren, N. J. Stam, C. Ohlen, J. J. Neefjes, P. Hoglund, M. T. Heemels, J. Bastin, T. N. Schumacher, A. Townsend, K. Karre, et al., *Nature* **1990**, *346*, 476-480.

[13] D. H. Fremont, M. Matsumura, E. A. Stura, P. A. Peterson, I. A. Wilson, *Science* **1992**, *257*, 919-927.

[14] D. H. Fremont, E. A. Stura, M. Matsumura, P. A. Peterson, I. A. Wilson, *Proc Natl Acad Sci U S A* **1995**, *92*, 2479-2483.

[15] K. L. Kiick, R. Weberskirch, D. A. Tirrell, *FEBS Lett* **2001**, *502*, 25-30.

[16] K. Udaka, K. H. Wiesmuller, S. Kienle, G. Jung, P. Walden, *J Biol Chem* **1995**, *270*, 24130-24134.

[17] T. Mareeva, E. Martinez-Hackert, Y. Sykulev, *J Biol Chem* **2008**, *283*, 29053-29059.

[18] P. Shieh, V. T. Dien, B. J. Beahm, J. M. Castellano, T. Wyss-Coray, C. R. Bertozzi, *J Am Chem Soc* **2015**, *137*, 7145-7151.

[19] J. Mahmoudian, R. Hadavi, M. Jeddi-Tehrani, A. R. Mahmoudi, A. A. Bayat, E. Shaban, M. Vafakhah, M. Darzi, M. Tarahomi, R. Ghods, *Cell Journal (Yakhteh)* **2011**, *13*, 169-172.

[20] D. H. Fremont, E. A. Stura, M. Matsumura, P. A. Peterson, I. A. Wilson, *Proceedings of the National Academy of Sciences of the United States of America* **1995**, *92*, 2479-2483.

[21] P. van Endert, *Immunol Rev* **2016**, *272*, 80-96.
[22] S. C. Jameson, M. J. Bevan, *Eur J Immunol* **1992**, *22*, 2663-2667.
[23] A. I. Webb, N. A. Borg, M. A. Dunstone, L. Kjer-Nielsen, T. Beddoe, J. McCluskey, F. R. Carbone, S. P. Bottomley, M.-I. Aguilar, A. W. Purcell, J. Rossjohn, *The Journal of Immunology* **2004**, *173*, 402-409.
[24] M. J. Miley, I. Messaoudi, B. M. Metzner, Y. Wu, J. Nikolich-Zugich, D. H. Fremont, *J Exp Med* **2004**, *200*, 1445-1454.
[25] P. Marrack, R. Shimonkevitz, C. Hannum, K. Haskins, J. Kappler, *The Journal of experimental medicine* **1983**, *158*, 1635-1646.
[26] A. Mortellaro, M. Urbano, S. Citterio, M. Foti, F. Granucci, P. Ricciardi-Castagnoli, *Methods Mol Biol* **2009**, *531*, 17-27.
[27] R. C. Su, R. G. Miller, *Journal of Immunology* **2001**, *167*, 4869-4877.
[28] E. Abbe, *Archiv für mikroskopische Anatomie* **1873**, *9*, 413-418.
[29] aS. van de Linde, M. Heilemann, M. Sauer, *Annu Rev Phys Chem* **2012**, *63*, 519-540; bA. Rasmussen, V. Deckert, *Anal Bioanal Chem* **2005**, *381*, 165-172.
[30] aB. Huang, M. Bates, X. Zhuang, *Annu Rev Biochem* **2009**, *78*, 993-1016; bD. van der Zwaag, N. Vanparijs, S. Wijnands, R. De Rycke, B. G. De Geest, L. Albertazzi, *ACS Appl Mater Interfaces* **2016**, *8*, 6391-6399.
[31] aL. Albertazzi, D. van der Zwaag, C. M. Leenders, R. Fitzner, R. W. van der Hofstad, E. W. Meijer, *Science* **2014**, *344*, 491-495; bR. M. da Silva, D. van der Zwaag, L. Albertazzi, S. S. Lee, E. W. Meijer, S. I. Stupp, *Nat Commun* **2016**, *7*, 11561.
[32] R. Han, Z. Li, Y. Fan, Y. Jiang, *J Genet Genomics* **2013**, *40*, 583-595.
[33] M. J. Rust, M. Bates, X. Zhuang, *Nat Methods* **2006**, *3*, 793-795.
[34] aJ. Herz, J. Pardo, H. Kashkar, M. Schramm, E. Kuzmenkina, E. Bos, K. Wiegmann, R. Wallich, P. J. Peters, S. Herzig, E. Schmelzer, M. Kronke, M. M. Simon, O. Utermohlen, *Nat Immunol* **2009**, *10*, 761-768; bD. M. van Elsland, E. Bos, W. de Boer, H. S. Overkleeft, A. J. Koster, S. I. van Kasteren, *Chemical Science* **2016**, *7*, 752-758.
[35] Z. Shen, G. Reznikoff, G. Dranoff, K. L. Rock, *J Immunol* **1997**, *158*, 2723-2730.
[36] C. P. Ramil, Q. Lin, *Chem Commun* **2013**, *49*, 11007-11022.
[37] S. I. van Kasteren, H. B. Kramer, H. H. Jensen, S. J. Campbell, J. Kirkpatrick, N. J. Oldham, D. C. Anthony, B. G. Davis, *Nature* **2007**, *446*, 1105-1109.
[38] J. W. Chin, S. W. Santoro, A. B. Martin, D. S. King, L. Wang, P. G. Schultz, *Journal of the American Chemical Society* **2002**, *124*, 9026-9027.
[39] aA. Deiters, T. A. Cropp, M. Mukherji, J. W. Chin, J. C. Anderson, P. G. Schultz, *Journal of the American Chemical Society* **2003**, *125*, 11782-11783; bW. Liu, A. Brock, S. Chen, S. Chen, P. G. Schultz, *Nature Methods* **2007**, *4*, 239-244.
[40] M. S. Siegrist, S. Whiteside, J. C. Jewett, A. Aditham, F. Cava, C. R. Bertozzi, *ACS chemical biology* **2012**, *8*, 500-505.
[41] F. Kotsias, E. Hoffmann, S. Amigorena, A. Savina, *Antioxidants & redox signaling* **2013**, *18*, 714-729.
[42] R. Singh, P. Cresswell, *Science* **2010**, *328*, 1394-1398.
[43] aD. H. Schuurhuis, S. Laban, R. E. M. Toes, P. Ricciardi-Castagnoli, M. J. Kleijmeer, E. I. H. van der Voort, D. Rea, R. Offringa, H. J. Geuze, C. J. M. Melief, F. Ossendorp, *The Journal of Experimental Medicine* **2000**, *192*, 145-150; bC. Winzler, P. Rovere, M. Rescigno, F. Granucci, G. Penna, L. Adorini, V. S. Zimmermann, J. Davoust, P. Ricciardi-Castagnoli, *The Journal of Experimental Medicine* **1997**, *185*, 317-328.
[44] A. Rhule, B. Rase, J. R. Smith, D. M. Shepherd, *J Ethnopharmacol* **2008**, *116*, 179-186.

[45] M. C. Feltkamp, H. L. Smits, M. P. Vierboom, R. P. Minnaar, B. M. de Jongh, J. W. Drijfhout, J. ter Schegget, C. J. Melief, W. M. Kast, *European Journal of Immunology* **1993**, *23*, 2242-2249.

[46] S. Khan, M. S. Bijker, J. J. Weterings, H. J. Tanke, G. J. Adema, T. van Hall, J. W. Drijfhout, C. J. M. Melief, H. S. Overkleeft, G. A. van der Marel, D. V. Filippov, S. H. van der Burg, F. A. Ossendorp, *J. Biol. Chem.* **2007**, M701705200.

[47] A. Neisig, J. Roelse, A. J. Sijts, F. Ossendorp, M. C. Feltkamp, W. M. Kast, C. J. Melief, J. J. Neefjes, *J Immunol* **1995**, *154*, 1273-1279.